Determination of Spiropyran Cytotoxicity by High Content Screening and Analysis for Safe Application in Bionanosensing

Dania Movia,[†,‡,⊥] Adriele Prina-Mello,[†,§,⊥] Yuri Volkov,[†,∥] and Silvia Giordani*[,†,‡]

Centre for Research on Adaptive Nanostructures and Nanodevices (CRANN), School of Chemistry, School of Physics, and School of Medicine, Trinity College Dublin, Dublin, Ireland

Received March 31, 2010

The *in vitro* toxic response of spiropyrans in cellular models has not been previously addressed, despite the fact that such photoswitchable molecules have shown great potential as versatile and tunable components for bionanodevices and imaging agents. In this study, we examine the cytotoxic effects of a spiropyran, namely, 8-methoxy-6-nitro-BIPS (1′,3′-dihydro-1′-ethanol-3′,3′-dimethyl-8-methoxy-6-nitrospiro(2*H*-1-benzopyran-2,2′-(2*H*)-indole) [**1**], in three cultured cellular models (THP-1, AGS, and A549 cell lines) by High Content Screening and Analysis (HCSA) and by enzyme-linked immunosorbent (ELISA) assays (Interleukin-6 and Tumor Necrosis Factor-alpha). The HCSA results show that low concentrations of 8-methoxy-6-nitro-BIPS (10^{-6}, 10^{-8}, and 10^{-9} M) do not induce any cytotoxic response after 24 and 72 h exposure time, while at the highest concentrations ($10^{-3}$and 10^{-4} M) the exposure time becomes a critical parameter of the toxic response. The cell viability is reduced by 60% for THP-1 cells, 50% for AGS cells, and 40% for A549 cells at a spiropyran concentration of 10^{-3} M after 24 h incubation, whereas at 72 h, the cell loss increases above 90%. Interestingly, at 10^{-4} M no significant cytotoxic response is registered after 24 h exposure, where contrarily cytotoxicity is verified after 72 h. Our ELISA results show that consistently with the HCSA analysis a robust inflammatory response is present at 10^{-3} M after 24 h exposure and at 10^{-3} M and 10^{-4} M after 72 h, in all three cell lines investigated.

Introduction

Since the discovery of spiropyrans in 1952 (*1*), researchers have investigated these compounds for various applications. Spiropyrans are molecular switches that can be reversibly converted between two or more stable states in response to stimuli (*1*). They may exist in three different forms: the colorless closed or spiro form (SP[1]), the highly conjugated colored open form referred to as merocyanine (ME), and the protonated open form (MEH). Switching among these three states is possible upon irradiation with UV and visible light and by the addition of an acid or a base (*2*−*4*).

As a result of their ability to alter their structural conformation in response to various photochemical stimuli, growing interest in the application of spiropyrans has been driven toward the selective chelation or release of certain metal-ions (*5*), imaging in living cells by an optical lock-in detection (OLID) approach (*6, 7*), and stimulated emission depletion (STED) microscopy (*8*). More recently, these molecules have been integrated in nanometer-sized molecular machines (*9, 10*), showing that such compounds have also considerable potential for biological applications as light-controlled nanosensors, drug delivery nanosystems (*11*), and nanofluidic systems (*12*). It has been reported, for example, that the opening/closing process of a nanovalve derived from a channel protein (*10, 12*), which was covalently modified with a spiropyran, can be controlled by light and might be used to drive molecules across the compartments of a nanodevice.

With the rapid growth of research toward the development of nanosystems, there has been a strong drive from both the International and European regulatory organizations to identify the methodologies for the assessment of the "Health, Safety and Environmental impact" of the new nanotechnologies (*13*). The Registration, Evaluation, Authorisation and Restriction of Chemicals (REACH) regulates and assesses the toxicity of all chemicals sold in Europe in large quantities (*14*). However, in 2008, the Organization for the Economic Co-operation and Development (OECD) expressed its concern on the relative inadequacy of toxicological data available on the new bionanotechnologies and all their fundamental constituents (*15*). To date, the main uncertainties regarding the potential integration of spiropyrans in nanoactuators, as well as their application as imaging agents, are related to their chemical instability in an aqueous environment (*16*) and to the lack of data on the toxicity or cytotoxicity attributed to these molecules. In fact, to date, the only toxicity information available comes from the Materials Safety Data Sheet (MSDS) for 6-nitro-BIPS [**2**] (Scheme 2), a compound commercially available from Sigma-Aldrich (CAS No.: 1498-88-0), which demonstrates a 50% lethal dose (LD_{50}) of 56 mg/kg by intravenous administration in mice.

In compliance with the aforementioned OECD directives and the scarcity of toxicological data on spiropyrans, this study aims to investigate whether the functional condition of macrophages

* Corresponding author. Tel: +353-1-896-1422. Fax: +353-1-671-2826. E-mail: giordans@tcd.ie.

[†] Centre for Research on Adaptive Nanostructures and Nanodevices (CRANN).

[‡] School of Chemistry.

[§] School of Physics.

[∥] School of Medicine.

[⊥] These authors contributed equally to this work.

[1] Abbreviations: AGS, human gastric cancer cell line; A549, human adenocarcinomic epithelial cell line; ELISA, enzyme-linked immunosorbent assay; HCSA, high content screening and analysis; IL-6, Interleukin-6; ME, merocyanine; MEH, protonated merocyanine; MSDS, Materials Safety Data Sheet; OECD, Organization for the Economic Co-operation and Development; REACH, Registration, Evaluation, Authorisation and Restriction of Chemicals; SP, spiropyran; THP-1, human monocytic leukemia cell line; TNF-α; Tumor Necrosis Factor-alpha.

10.1021/tx100123g
Published on Web 09/01/2010

Scheme 1. Isomeric Forms of 8-Methoxy-6-nitro-BIPS [1][a]

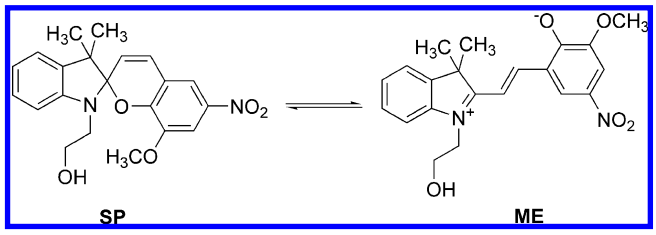

[a] On the right is molecular structure of the colored merocyanine form (ME). In water, the molecule can be switched to the colorless closed form (SP) upon vis irradiation.

Scheme 2. Molecular Structures of 6-Nitro-BIPS [2]

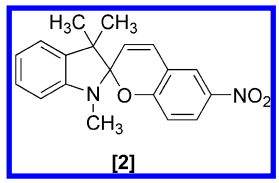

(THP-1 cell line), gastric cells (AGS cell line), and epithelial cells (A549 cell line) could be significantly altered by the exposure to 8-methoxy-6-nitro-BIPS [**1**] (Scheme 1) (*17*). The objective of this work is two fold: (i) the investigation of the chemical stability of the spiropyran [**1**] in an aqueous environment by optical spectroscopy; and (ii) the evaluation of the dose- and time-dependent cytotoxic response to this photochromic compound in various cultured cell models. Since access to the human body can occur through skin absorption (and consequent perfusion into the systemic blood circulation), ingestion, and/or inhalation (*18*), THP-1, AGS, and A549 cell lines were chosen as the most suitable models to investigate the potential toxicity associated with the use of 8-methoxy-6-nitro-BIPS [**1**] as chemical nanosensor and/or component of functioning nanomachines (*18*). Five different concentrations of spiropyrans ranging from 10^{-3} M to 10^{-9} M were prepared and tested at two end points set at 24 and 72 h.

We chose the HCSA system as the ideal tool in multiparametric evaluation of cellular responses, such as viability, membrane permeability, lysosomal mass/pH changes, and nuclear staining intensity/size, using established fluorescent biomarkers (*19*). The HCSA system is becoming increasingly important as a powerful tool for the screening of large sets of drug candidates (*20*−*22*), nanoparticles (*23*−*25*), and nanostructures (*26*) for both efficacy and toxicity. Since responses to external agents are commonly not limited to a single cellular target or isolated mechanisms of interaction (*27*), HCSA provided a reliable and reproducible system for the toxicity screening of the selected molecular switch.

To further corroborate the HCSA multiparameter results presented, parallel ELISA assays were carried out on the relevant (glycol-) protein signaling molecules (cytokines). The ELISA assay allowed us to quantify the extent of protein secretion related to the cell stress-induced signaling cascade and transduction activity induced by the exposure of the three cellular models to the 8-methoxy-6-nitro-BIPS [**1**].

Experimental Procedures

Optical Studies. Synthesis, purification, and the X-ray crystal structure of 1′,3′-dihydro-1′-ethanol-3′,3′-dimethyl-8-methoxy-6-nitro-spiro(2*H*-1-benzopyran-2,2′-(2*H*)-indole) (8-methoxy-6-nitro-BIPS) [**1**] (Scheme 1) have been reported previously (*17*). 8-Methoxy-6-nitro-BIPS [**1**] was dispersed in Milli-Q water by sonication at a concentration of 10^{-3} M. The solution at 10^{-4} M was obtained by dilution with fresh Milli-Q water. The solution was incubated at 37 °C in the dark up to 72 h; it showed a neutral pH before and after spectroscopic experiments. UV/vis absorption measurements were carried out in accordance with the *in vitro* incubation conditions (37 °C, 3 time points), with PerkinElmer UV/vis Lambda 35 Absorption Spectrophotometer. Further absorption spectra were collected following cycles of vis (878 nm) and UV (254 nm) irradiation. The vis emission spectra were recorded on PerkinElmer LS 55 Emission Spectrophotometer at an excitation wavelength (λ_{exc}) of 530 nm.

Spiropyran Solutions in Cell Media. 8-Methoxy-6-nitro-BIPS [**1**] was added to RPMI 1640 cell media (GIBCO, Invitrogen, USA) or Hams F12 media (GIBCO, Invitrogen, USA) in a sterile environment at a concentration of 10^{-3} M. The dispersion was sonicated for 7 h in a sonic bath in order to obtain a homogeneous solution. All of the other concentrations (10^{-4}, 10^{-6}, 10^{-8}, and 10^{-9} M) were obtained by progressive dilutions with fresh cell media. For all of the concentrations, neutral pH was measured.

Cell Culture. Three established commercially available cell lines (all from ATCC, VA, USA) were used: human monocytic leukemia cell line (THP-1), human gastric cancer cell line (AGS), and human alveolar epithelial cell line (A549). Full cell line characterization (e.g., cell line profile, morphological images, DNA profile, and cytogeneticity), subculturing, propagation, doubling time, and preservation were also supplied by ATCC at the delivery. The passage number was restricted between five and eight.

THP-1 Cells. The human monocytic leukemia cell line (THP-1 cell line) was cultured in modified RPMI 1640 media (supplemented with streptomycin, penicillin, and L-glutamine) in T75 tissue culture flasks and incubated at 37 °C and 5% CO_2 until a 60% confluence was reached. THP-1 cells were seeded in a 96-wells plate at a concentration of 20,000 cells/well (final volume: 200 μL/well) using a Matrix WellMate (ThermoFisher Scientific, USA) and activated with phorbol-12-myristate-13-acetate (PMA) (Sigma-Aldrich, USA) for 72 h to induce their differentiation into adherent macrophages and stop their natural proliferation.

AGS Cells. The human gastric cancer cell line (AGS cell line) was cultured in modified Hams F12 media (supplemented with 1% penicillin/streptomycin and 10% fetal bovine serum) in T75 tissue culture flasks and incubated at 37 °C and 5% CO_2 until a 70−80% confluence was reached. AGS cells were seeded in a 96-wells plate at aconcentration of 4,000 cells/well (final volume: 200 μL/well) using a Matrix WellMate (ThermoFisher Scientific, USA) and incubated at 37 °C and 5% CO_2 for 24 h for complete adhesion. Different from the THP-1 cells, this cell line was distinguished by cellular proliferation during the entire experiment.

A549 Cells. Human alveolar epithelial adenocarcinomic cells (A549 cell line) were cultured in modified Hams F12 media (supplemented with 1% penicillin/streptomycin and 10% fetal bovine serum) in T75 tissue culture flasks and incubated at 37 °C and 5% CO_2 until a 70−80% confluence wa reached. A549 cells were seeded in a 96-wells plate at a concentration of 4,000 cells/well (final volume: 200 μL/well) using a Matrix WellMate (ThermoFisher Scientific, USA) and incubated at 37 °C and 5% CO_2 for 24 h for complete adhesion. Similar to AGS cells, this cell line was distinguished by cellular proliferation during the entire experiment.

Cytotoxicity Methodology. After removing the cell media, adherent THP-1, AGS and A549 cells were exposed to spiropyran [**1**] solutions prepared with fresh cell media. The final volume of solution added was 300 μL/well. To assess the dose-dependent cytotoxicity, the experiment design consisted of a total of five different doses (10^{-3}, 10^{-4}, 10^{-6}, 10^{-8}, and 10^{-9} M), one negative control (cells plated with cell media) and one positive control, in triplicate wells. Detergent damage (Triton-X 0.05%) was used as the positive control in the THP-1 cell line, while an anticancer drug (Pacliataxel 4 μM) was used as the positive control in AGS and A549 cells. The exposure times chosen for each experiment were 24 and 72 h, to assess the time-dependent cytotoxicity. Positive and negative controls, temperature, and pH were controlled and kept constant across the experiments.

Table 1. Summary of the Assay Strategy for Measuring the Cellular Parameters of Interest by HCSA[a]

cellular parameter	description	target	model of action	fluorescence emission
cell count	number of nuclei identified per field	nucleus	DNA binding	blue (λ_{em}: 461 nm)
cell membrane permeability	average fluorescence intensity of pixels within the cytoplasm	cell membranes	cell membrane is permeable when compromised	green (λ_{em}: 509 nm)
lysosomal mass/pH changes	average fluorescence intensity of pixels within the cytoplasm	acid organelles	increase fluorescence corresponds to decreased pH or increased lysosomes number	red (λ_{em}: 599 nm)
nuclear intensity	average fluorescence intensity of pixels within nucleus	nucleus	DNA binding	blue (λ_{em}: 461 nm)
nuclear area	number of pixels within the nucleus	nucleus	DNA binding	blue (λ_{em}: 461 nm)

[a] This description is in agreement with previously published work (*24*).

Live Fluorescent Staining. Supernatants were collected from each well for postexposure assays, and Multiparameter Cytotoxicity 1 HitKit HCSA Reagent Kit (Cat. No.: 8400101, ThermoFisher, USA) was used for staining the three cell lines following the optimized Kit procedure provided for live cell staining (the detailed protocol is reported in Supporting Information). Cytotoxicity 1 HitKit is formed by a cocktail of three fluorescent dyes (MPCT1 Fluor Cocktail), which contain the following components: (i) Hoechst Dye (blue dye) for labeling nuclei; (ii) cell permeability indicator (green dye) for labeling permeabilized cells; and (iii) fluorescent weak base (red dye) for labeling acidic organelles and measuring pH and mass. This kit offers, therefore, the ability to detect changes to many cellular properties, such as (i) cell viability (determined as cell loss compared to the negative controls); (ii) cell membrane permeability; (iii) lysosomal mass/pH changes; (iv) nuclear DNA staining intensity; (v) nuclear size; and (vi) cellular morphology. A complete list of the parameters acquired in this study, along with explanations, is given in Table 1.

Imaging and Multiparametric Analysis. Measurements were carried out using the IN-Cell 1000 automated fluorescent microscope system (GE Healthcare, USA) and its associated analysis software (In Cell Analyzer System, GE Healthcare, USA). 96-wells plates prepared as described above were read on IN-Cell Analyzer 1000 using three detection channels with three different excitation filters. These included a $\lambda < 503$ nm filter, which detected the blue fluorescence at 461 nm; a $\lambda > 509$ nm filter, which detected the green fluorescence at 509 nm; and a $\lambda > 599$ nm filter, which detected the red fluorescence at 599 nm. Ten random microscopic fields were sequentially acquired by the IN-Cell 1000 automated fluorescent microscope system at a magnification of 10×, after carrying out image calibration and maintaining constant the acquisition time, contrast, and brightness throughout the experiment. Acquired images for each exposure time and dose were then analyzed by the IN-Cell Analyzer software, which automatically identifies objects based on a fluorescent stain following calibration on the control samples. To obtain the cell viability data, an algorithm-based software analysis was applied to detect and count the stained nuclei (blue channel) per field. From the microscopic fields, the fluorescent staining intensities reflecting cell permeability (green channel) and lysosomal mass/pH changes (red channel) were also quantified for each individual cell present in the fields, by means of the analysis software. Further algorithms were applied to measure the average intensity (nuclear intensity) and the intensity distribution (nuclear area) of blue pixels confined within the nuclear outline.

Cytokine Assays. To correlate the cytotoxicity with the downstream functional responses at the level of protein secretion, the concentrations of natural human Interleukin-6 (IL-6) and human Tumor Necrosis Factor-alpha (TNF-α) secreted by the exposed THP-1, AGS, and A549 cells were measured (human TNF-α/TNFSF1A, catalog number,: DY210; human IL-6, catalog number, DY206; DuoSet ELISA Development kit, R&D Systems). Cell cytokines expression due to the exposure to spiropyran [**1**] was evaluated by ELISA assays and compared to the relevant controls, following the standard procedure (Supporting Information). The assays were repeated in duplicate ($n_{test} = 2$). The optical density of each well at 450 nm was determined by means of a VERSAMax Plus microplate reader (Molecular Devices, USA), calibrated against standards and corrected by subtracting the optical aberration of the 96-wells plastic plate. The cell count for each well was carried out by the HCSA system in order to quantify the cytokine production as picogram per cell (pg/cell) for the different concentrations and time points.

Statistical Analysis. A two-way analysis of variance (ANOVA) followed by a Bonferroni post-test analysis were carried out for all HCSA and cytokine parameters to measure the significance of dose- and time-interdependencies between the negative controls and the five spiropyran concentrations chosen in this study (Prism; GraphPad Software Inc., USA). $p < 0.05$ was considered statistically significant. A comprehensive list of the p values at each concentration and time point has been summarized in Tables S1−S5 in Supporting Information. The HCSA data are presented in the graphs as mean values ($n_{test} = 3$ in THP-1 cells; $n_{test} = 2$ in AGS and A549 cells; $n_{replicates} = 3$ in all cell lines) ± standard error of the mean and normalized to the negative control cells, unless differently specified in the graph caption. The histograms showing the ELISA results are plotted as mean values ($n_{test} = 2$) ± standard error of the mean.

Results

Optical Studies. We monitored the stability of 8-methoxy-6-nitro-BIPS [**1**] in water, after the incubation of the aqueous solution at 37 °C and at various time points (0, 24, and 72 h) by optical spectroscopy.

The absorption spectrum of the spiropyran derivative [**1**] in aqueous solution (black solid line in Figure 1A) showed two bands at 390 and 526 nm, revealing the presence of the open merocyanine form, confirmed by an emission band at 688 nm (black dashed line in Figure 1A). The absorption and emission spectra did not change much after storing the solutions for 24 h at 37 °C (gray solid and dashed lines in Figure 1A), while significant spectroscopic changes were recorded after 72 h. The intensity of the absorption band at 526 nm and the emission band at 688 nm dramatically decreased, and four new absorptions bands appeared at 263 nm, 305 nm, 374 nm, and 413 nm, indicating decomposition of the spiropyran derivative after 72 h storage of the aqueous solution at 37 °C. In particular, the small absorption band at 305 nm was assigned to the 5-nitrosalicylaldehyde generated by the decomposition of 8-methoxy-6-nitro-BIPS [**1**] (*16*).

The absorbance at 526 nm can be modulated by alternating visible and UV radiations. The data points in Figure 1B illustrate this effect for three consecutive switching cycles.

The dynamic switching between ME (fluorescent form) and SP (nonfluorescent form) in water was seen under an epifluorescent microscope ($\lambda_{exc} = 450$ nm; $\lambda_{em} = 596$ nm; CCD camera, Olympus BX501M, Japan) by live imaging of a freshly

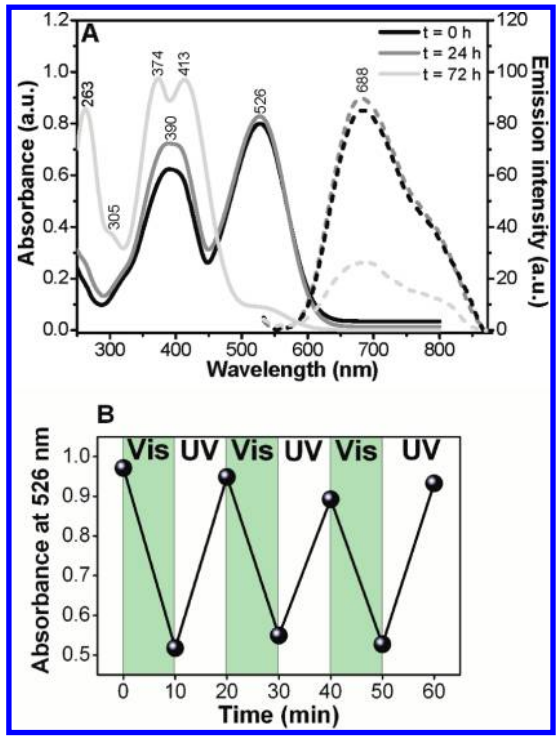

Figure 1. (A) Absorption (solid lines) and emission spectra (dashed lines) of [**1**] (10^{-4} M, water, 37 °C) after 0, 24, and 72 h of incubation. (B) Changes in absorbance at 526 nm under the influence of visible and UV light for three consecutive cycles.

prepared aqueous solution of 8-methoxy-6-nitro-BIPS [**1**] (the video is available in Supporting Information).

High Content Screening and Analysis. The cytotoxic outcomes of the cell−spiropyran [**1**] interaction were evaluated by HCSA in three cellular models (THP-1, AGS, and A549 cells) after 24 and 72 h exposure. The evaluation of the HCSA images acquired (Figure 2 and Figure S1, Supporting Information), showed that the cytotoxic response to 8-methoxy-6-nitro-BIPS [**1**] was both dose- and time-dependent. The multiparametric analysis provided quantitative information on the changes in five commonly used cellular parameters (*20, 22*−*26*), including cell viability, membrane permeability, lysosomal mass/pH changes, nuclear area, and nuclear staining intensity, as explained in detail in Table 1. The quantitative results are shown in Figure 3 and in Figure S2 (in Supporting Information).

Cell Viability. By assuming that changes in cell viability are directly correlated to the toxic effects of the compound tested, we found that 8-methoxy-6-nitro-BIPS [**1**] did not affect the cellular survival of THP-1, AGS, and A549 cells at 24 h, for concentrations ranging from 10^{-4} M to 10^{-9} M (Figure 3A, D, and G). However, at 10^{-3} M a significant decrease in cell viability down to 40%, 50%, and 60% was shown for THP-1, AGS, and A549 cells, respectively, when compared to negative controls. At 72 h, we found a further decrease in cell viability down to 20% at 10^{-3} M in all cell lines. At 10^{-4} M, the cytotoxic responses to spiropyran [**1**] were cell type-dependent at 72 h. THP-1 cells showed an overall cell loss of 40%, while AGS and A549 cells had a reduction of approximately 50% in their proliferative activity. For all the other concentrations, the cell−spiropyran interactions at 72 h were found to be negligible across the three cell lines investigated. This was reflected by the 100% viability of the THP-1 cells, and the 3-fold increase in cell number of both AGS and A549, as a clear indication of their normal proliferation.

The dose-dependent cell loss was found to be significant at 10^{-3} M in THP-1 cells and at 10^{-3} M and 10^{-4} M in AGS cells. Significant time-dependent cell viability changes were shown at 10^{-3} M and 10^{-4} M in the AGS cell line and at 10^{-3}

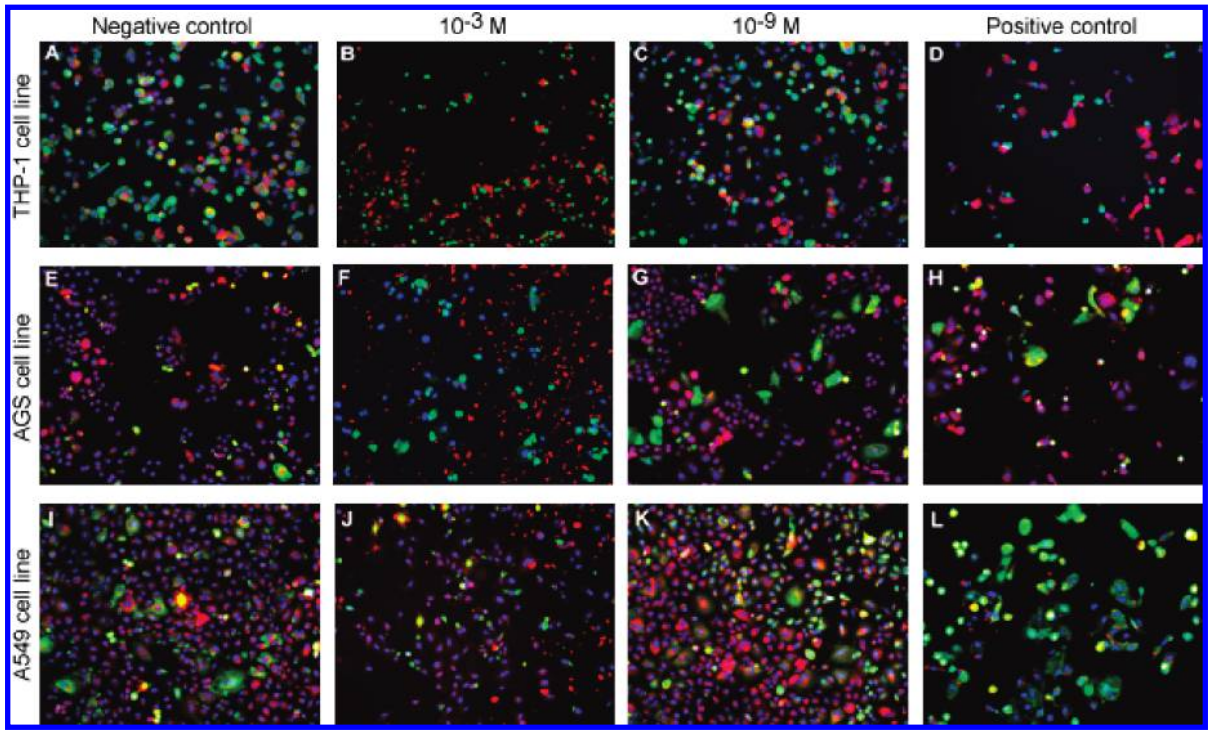

Figure 2. HCSA qualitative results for THP-1 cells (A−D), AGS cells (E−H), and A549 cells (I−L) at 24 h of exposure to the spiropyran derivative [**1**]. The composite images show the cells stained for (i) nuclei (in blue); (ii) cell membrane permeability (in green); and (iii) lysosomal mass/pH changes (in red). The results for two representative concentrations (10^{-3} M and 10^{-9} M) are reported. Panels B, F, and J are significant image fields showing decreased cell viability and increased cell membrane permeability at 10^{-3} M, as compared to the negative controls (panels A, E, and I). The cell viability results comparable to the negative controls at 10^{-9} M (panels C, G, and K). Panels D, H, and L are significant fields of the positive controls. Image size: 0.897 mm × 0.671 mm (10× objective).

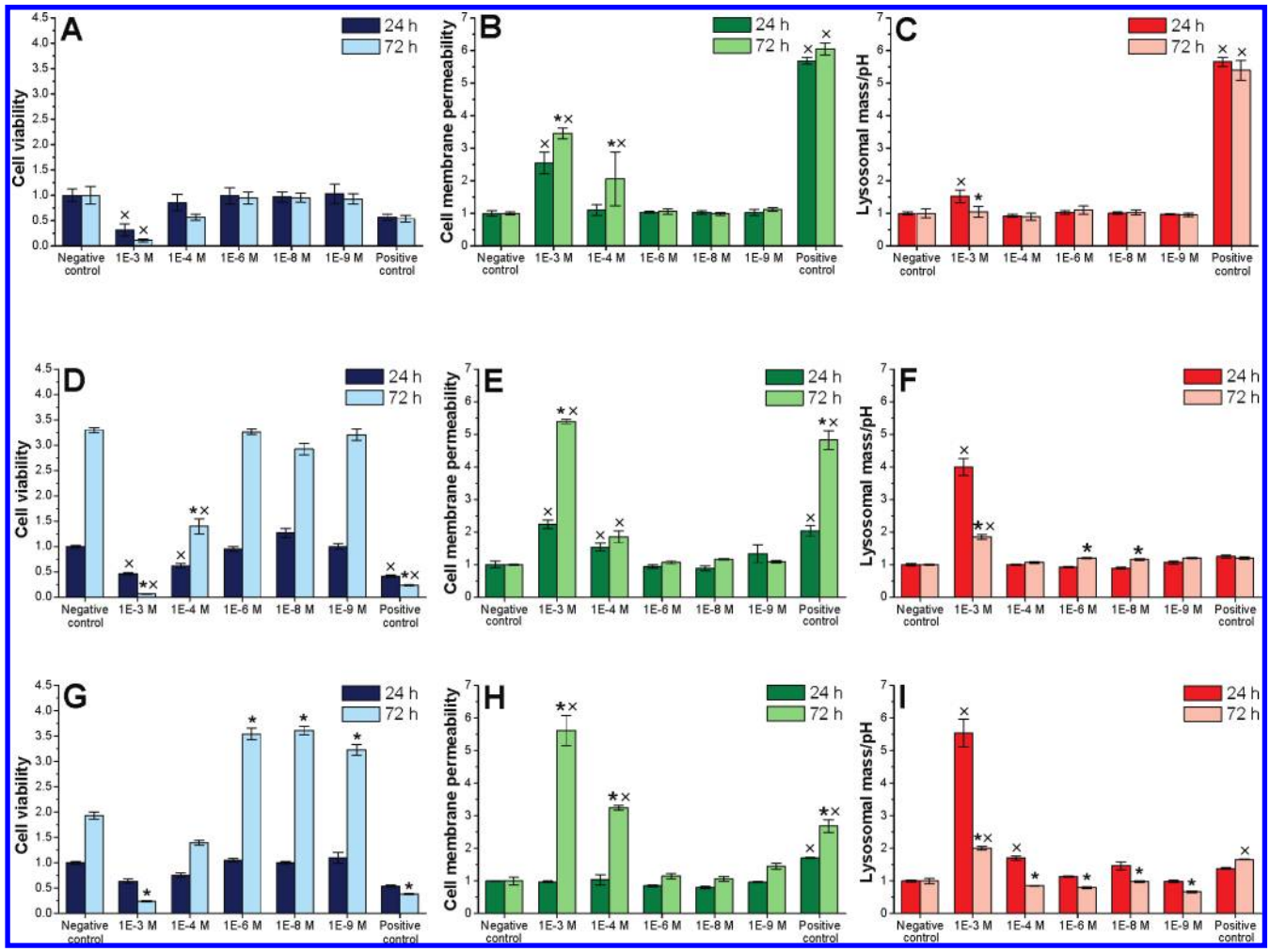

Figure 3. HCSA quantitative results for THP-1, AGS, and A549 cells to the spiropyran derivative [**1**] at five different concentrations (10^{-3}, 10^{-4}, 10^{-6}, 10^{-8}, and 10^{-9} M) for two end points (24 and 72 h). In blue, dose- and time-response of (A) THP-1, (D) AGS, and (G) A549 cell population viability to spiropyran exposure; the data are normalized to the negative control at 24 h. In green, cell membrane permeability changes of (B) THP-1, (E) AGS, and (H) A549 cells associated with the exposure to spiropyran; the data for each time point are normalized to the matching negative control. In red, lysosomal mass/pH changes of (C) THP-1, (F) AGS, and (I) A549 cells associated with the exposure to spiropyran are shown; the data for each end point are normalized to the matching negative control. The symbol (×) above the bars indicates dose-dependent cytotoxicity as compared to the negative controls (two-way ANOVA, $p < 0.05$), while the symbol (*) indicates statistically significant time-dependent cytotoxicity (two-way ANOVA, $p < 0.05$).

M, 10^{-6} M, 10^{-8} M, and 10^{-9} M in A549 cells, as summarized in Tables S1, S2, and S3 (Supporting Information).

Cell Membrane Permeability. It has been reported that changes in cell membrane permeability are often associated with an ongoing toxic or apoptotic responses, and the loss of cell membrane integrity is a common phenotypic feature of marked cytotoxicity (*28*). We used this as a key parameter for the evaluation of the cell−spiropyran interaction in addition to the cell viability.

A significant increase in the cell membrane permeability (evaluated by green-fluorescence emission) was registered at 10^{-3} M at 24 h and at 10^{-3} M and 10^{-4} M at 72 h, in all cellular models tested (as shown in Figure 3B, E, and H for THP-1, AGS, and A549 cells, respectively). Interestingly, for the AGS cell model, an onset of toxicity, shown by increased cell membrane permeability, was measured at 10^{-4} M after only 24 h exposure; this response was not registered for any other cell lines tested in this study.

The dose-dependent increment in cell membrane permeability was significant at 10^{-3} M and 10^{-4} M in THP-1, AGS, and A549 cells. The time-dependent changes in cell membrane permeability were prominent at 10^{-3} M in AGS cells, and at 10^{-3} M and 10^{-4} M in THP-1 and A549 cells.

Lysosomal Mass/pH Changes. Changes in the mass/pH of lysosomes were also investigated at 24 and 72 h (Figure 3C, F, and I) since it has been reported that external agents (such as drugs and nanoparticles) can interfere with the normal cell physiology, by affecting the mass, the number, and/or the function of lysosomes and endosomes (*29*). In our study, high values in the lysosomal mass/pH parameter (evaluated by the red-fluorescence emission within the cellular cytoplasm) may also be associated with the endocytosis of the small spiropyran molecules (mass wt = 382 g/mol) and subsequent hydrolysis and storage in the lysosomes.

For THP-1, AGS, and A549 cells, increasing values of lysosomal mass/pH were found at 10^{-3} M after 24 h exposure. Conversely, while increasing values were observed in A549 cells at concentrations ranging between 10^{-4} M and 10^{-9} M, at 24 h, the red fluorescence intensities were comparable to those of the untreated controls in THP-1 and AGS cell models. Interestingly, THP-1 cells showed no significant changes in their lysosomal mass/pH response after 72 h of exposure, whereas rising values of red-fluorescence intensity were still detected at 72 h, when 8-methoxy-6-nitro-BIPS [**1**] was incubated at 10^{-3} M in AGS and A549 cell lines. Furthermore, lysosomal mass/pH changes

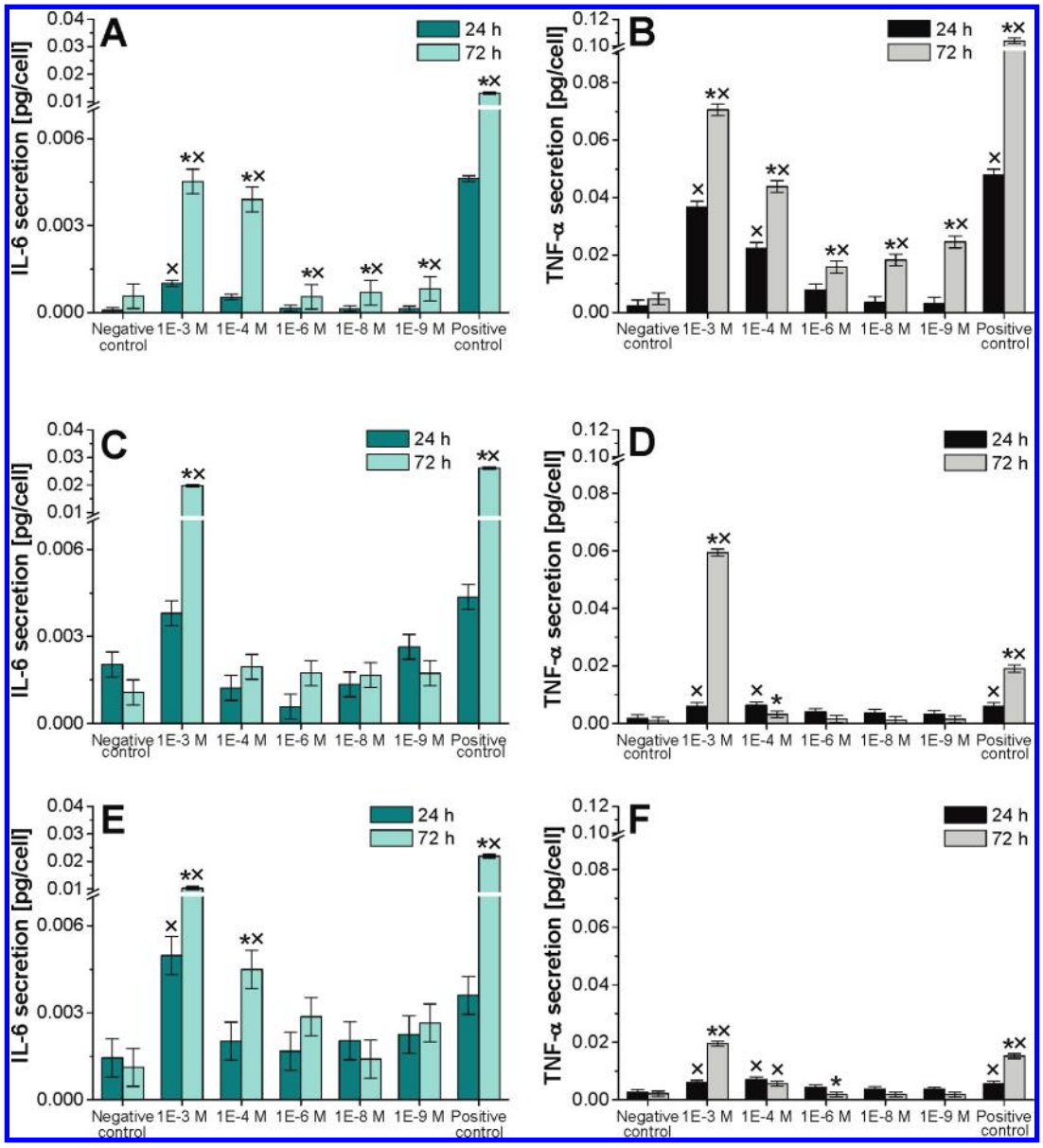

Figure 4. Concentration of pro-inflammatory cytokines released from (A,B) THP-1 cells, (C,D) AGS cells, and (E,F) A549 cells, after 24 and 72 h of incubation of five different concentrations of 8-methoxy-6-nitro-BIPS [**1**] (10^{-3}, 10^{-4}, 10^{-6}, 10^{-8}, and 10^{-9} M). In cyan, concentration of IL-6; in black, concentration of TNF-α. The data are represented as average ($n_{test} = 2$) ± SEM picograms (pg) per cell. The symbol (×) above the bars indicates dose-dependent cytotoxicity as compared to the negative controls (two-way ANOVA, $p < 0.05$), while the symbol (*) indicates statistically significant time-dependent cytotoxicity (two-way ANOVA, $p < 0.05$).

were also observed at 72 h in AGS and A549 cell lines across all the remaining concentrations (10^{-4} M to 10^{-9} M).

Dose-dependent lysosomal mass/pH changes were verified at 10^{-3} M in all cellular models tested. Time-dependent lysosomal mass/pH responses were significant at 10^{-3} M in all cell lines, at 10^{-6} M and 10^{-8} M in AGS cells and from 10^{-4} M to 10^{-6} M in A549 cells.

Nuclear Area and Intensity. The changes in nuclear area and nuclear staining intensity confirmed and strengthened the dose- and time-dependent cytotoxic trend showed by cell viability, cell membrane permeability, and lysosomal mass/pH changes (Figure S2, Supporting Information).

Cytokines Secretion. In the presence of an inflammogenic compound or a foreign body, THP-1, AGS, and A549 cells release inflammatory cytokines (*30*), the levels of which are clearly associated with cell-based inflammatory reactions (*31*). To refine the investigation on the dose- and time-response of THP-1, AGS, and A549 cells to spiropyran exposure, the secretion levels of IL-6 and TNF-α were measured on the supernatants of the exposed cells by ELISA assays. IL-6 and TNF-α are, in fact, multifunctional cytokines known to be secreted by cells to regulate their acute phase reactivity (*32*). The results on the concentrations of IL-6 and TNF-α secreted by THP-1, AGS, and A549 cells after 24 and 72 h of exposure to 8-methoxy-6-nitro-BIPS [**1**] are shown in Figure 4.

In THP-1 cells, the cytokine secretion levels were significantly high at 10^{-3} M at 24 h and at 10^{-3} M and 10^{-4} M at 72 h. This suggested that high concentrations and longer exposure times to 8-methoxy-6-nitro-BIPS [**1**] induced a pleiotropic inflammatory response, triggering the release of both cytokines by exposed THP-1 cells. At 72 h, the IL-6 and TNF-α secretion levels increased 2-fold. This phenomenon was due to the extended exposure exercised on the THP-1 cells, which triggered the onset of acute phase reaction. In AGS and A549 cells, high TNF-α concentrations were found at 10^{-3} M and 10^{-4} M at 24 h, and 10^{-3} M at 72 exposure. Furthermore, the secretion of IL-6 was prominent at 10^{-3} M at 24 h and outstanding at both 10^{-3} M and 10^{-4} M at 72 h.

IL-6 and TNF-α secretion levels were dose-dependent at 10^{-3} M in AGS cells and at 10^{-3} M and 10^{-4} M in the A549 cell line, as summarized in Tables S4 and S5 (Supporting Information). Interestingly, in THP-1 cells the secretion of IL-6 and TNF-α proved to be dose-dependent for all concentrations tested. The time-dependent IL-6 secretion was shown to be significant at 10^{-3} M in all three cell lines and at 10^{-4} M in A549 cells. TNF-α secretion was significantly time-dependent at 10^{-3} M in all three cell lines and at 10^{-4} M only in AGS cell lines.

Discussion

Several cellular parameters (such as cell viability, cell membrane permeability, lysosomal mass/pH changes, and nuclear DNA binding) were measured via the HCSA system. From the combined qualitative and quantitative HCSA analysis at 24 and 72 h exposure, it was possible to conclude that 8-methoxy-6-nitro-BIPS [**1**] was not cytotoxic for the three cellular models tested below a certain threshold. Thus, after 24 h, THP-1, AGS, and A549 cells were not significantly damaged at concentrations below or equal to 10^{-4} M. A clear cytotoxic effect was observed only at 10^{-3} M. At this concentration, the cell viability and the nuclear area consistently decreased in conjunction with a marked increase in cell membrane permeability. This phenomenon is generally associated with an ongoing dose-dependent cell insult. Similarly, time-dependent cytotoxicity was verified, as an increased cytotoxic response was registered at 10^{-4} M at 72 h exposure in all three cell lines. At this concentration and time point, the cell viability and nuclear area decreased when compared to the results at 24 h, while the cell membrane permeability and nuclear intensity increased. This suggested that the cytotoxic event was predominantly determined by the exposure time rather than the immediate toxic effect of the products generated by the hydrolysis of 8-methoxy-6-nitro-BIPS [**1**]. It is of interest that at 10^{-4} M the cell viability remained above 50% for all cellular models investigated even after 72 h exposure. This clearly showed that THP-1, AGS, and A549 cells were relevantly resistant to the presence of high concentrations of 8-methoxy-6-nitro-BIPS [**1**].

HCSA also allowed for the detection of subtle differences in the cytotoxic response among the three cell lines tested. THP-1 cells showed clear changes in the lysosomal mass/pH at 10^{-3} M after 24 h exposure. This result, combined with the increase in nuclear staining and decreased nuclear area, lead us to speculate that THP-1 cells were undergoing endocytosis of the photochromic compound after initial exposure. Since changes in the lysosomal mass/pH were not shown after 72 h, it is possible that such uptake reached saturation levels after the first 24 h exposure and was exhausted after 72 h. A similar pattern could be seen in A549 cells, whereas AGS cells showed an increasing cell membrane permeability at 10^{-4} M after 24 h incubation. This result could define a relative sensitivity of AGS cells toward exposure to 8-methoxy-6-nitro-BIPS [**1**], but it was not supported by analogous changes in the other parameters analyzed.

The data obtained from the cytokine assays corroborated the HCSA results and clearly showed that the pro-inflammatory cytokine production was both dose- and time-dependent. An overall remarkable inflammatory response of the three cellular models tested was seen at 10^{-3} M after 24 h exposure and at $10^{-3}$and 10^{-4} M after 72 h. From the results, it emerged that AGS and A549 cells secreted lower concentrations of TNF-α, as compared to THP-1 cells. These results also revealed that the inflammatory response of AGS and A549 cells to 8-methoxy-6-nitro-BIPS [**1**] was exhausted after 24 h exposure. This is in agreement with the physiological differences between the cellular models tested since, for instance, cytokines from the TNF family are mainly produced by macrophages. The secretion of both cytokines (TNF-α and IL-6) was found to be consistently dose-dependent.

In conclusion, we have demonstrated that strong toxic effects on macrophage, gastric, and epithelial cells are unlikely as a result of continuous exposure to the spiropyran at micromolar concentrations over a 72 h exposure period. Significant cytotoxic effects were found in fact only at 10^{-3} M after 24 h exposure and for longer exposures at 10^{-4} M. Using HCSA, we have shown that the dose- and time-dependent cytotoxic responses to 8-methoxy-6-nitro-BIPS [**1**] in THP-1, AGS, and A549 cells are statistically significant. Using ELISA assays, we have validated the HCSA system as a highly precise tool for further testing and screening the effects of spiropyrans in a larger range of cell types and exposure conditions. While our cytotoxicity study of a spiropyran clearly shows that such compounds have considerable promise as integral and active components in biologically relevant nanosensors, the optical studies indicate that the degradation process of 8-methoxy-6-nitro-BIPS [**1**] in water started after 24 h at 37 °C. Therefore, applications *in vivo* could still be limited by the hydrolysis of spiropyran or by the possible toxic effects of light-induced switching inside the cell. This work is a first step toward the screening of the *in vitro* cytotoxic response of switching spiropyrans inside the cell.

Acknowledgment. This work was supported by Science Foundation Ireland under different schemes (PIYRA 07/Y12/I1052, CSET, and SRC), Higher Education Authority (HEA) under the PRTLI-4 program, the Health Research Board, and IRCSET (Postgraduate Research Scholarship to D.M.). We are grateful to Dr. Despina Bazou for live imaging, Mr. Antoin Douglawi and Mr. Manuel Natali for the synthesis of spiropyran. We also thank Ms. Fiona Byrne, Dr. Anthony Davies, and Dr. Bashir Mohammed (TCD-HCSA laboratory) for technical support and fruitful discussions.

Supporting Information Available: Experimental methods and statistical analysis tables; nuclear area and nuclear intensity changes at 24 and 72 h exposure; HCSA qualitative results at 72 h exposure; and live imaging of a freshly prepared spiropyran aqueous solution by means of epifluorescent microscope. This material is available free of charge via the Internet at http://pubs.acs.org.

References

(1) Fischer, E., and Hirshberg, Y. (1952) Formation of colored forms of spiropyrans by low-temperature irradiation. *J. Chem. Soc.* 4522–4524.
(2) Raymo, F. M., and Giordani, S. (2001) Signal Processing at the Molecular Level. *J. Am. Chem. Soc. 123*, 4651–4652.
(3) Raymo, F. M., Giordani, S., White, A. J. P., and Williams, D. J. (2003) Digital processing with a three-state molecular switch. *J. Org. Chem. 68*, 4158–4169.
(4) Giordani, S., and Raymo, F. M. (2003) A switch in a cage with a memory. *Org. Lett. 5*, 3559–3562.
(5) Natali, M., Aakeroy, C. B., Desper, J. Giordani, S. (2010) The role of metal ions and counterions in the switching behavior of a carboxylic acid functionalized spiropyran. *Dalton Trans. 39*, 8269−8277.
(6) Marriott, G., Mao, S., Sakata, T., Ran, J., Jackson, D. K., Petchprayoon, C., Gomez, T. J., Warp, E., Tulyathan, O., Aaron, H. L., Isacoff, E. Y., and Yan, Y. L. (2008) Optical lock-in detection imaging microscopy for contrast-enhanced imaging in living cells. *Proc. Natl. Acad. Sci. U.S.A. 105*, 17789–17794.
(7) Mao, S., Benninger, R. K. P., Yan, Y. L., Petchprayoon, C., Jackson, D., Easley, C. J., Piston, D. W., and Marriott, G. (2008) Optical lock-in detection of FRET using synthetic and genetically encoded optical switches. *Biophys. J. 94*, 4515–4524.

(8) Seefeldt, B., Kasper, R., Beining, M., Mattay, J., Arden-Jacob, J., Kemnitzer, N., Drexhage, K. H., Heilemann, M. and, and Sauer, M. Spiropyrans as molecular optical switches. *Photochem. Photobiol. Sci. 9*, 213–220.
(9) Astier, Y., Bayley, H., and Howorka, S. (2005) Protein components for nanodevices. *Curr. Opin. Chem. Biol. 9*, 576–584.
(10) Kocer, A., Walko, M., Meijberg, W., and Feringa, B. L. (2005) A light-actuated nanovalve derived from a channel protein. *Science 309*, 755–758.
(11) Yoshida, M., and Lahann, J. (2008) Smart nanomaterials. *ACS Nano 2*, 1101–1107.
(12) Browne, W. R., and Feringa, B. L. (2006) Making molecular machines work. *Nat. Nanotechnol. 1*, 25–35.
(13) Commission of the European Communities (2009) *Nanosciences and Nanotechnologies: An action plan for Europe 2005−2009. Second Implementation Report 2007−2009*, Commission of the European Communities.
(14) (2006) *DIRECTIVE 2006/121/EC, Registration, Evaluation, Authorisation and Restriction of Chemicals (REACH)*.
(15) OECD (2008) Current developments/activities on the safety of manufactured nanomaterials, in *Environment, Health and Safety Publications: Series on the Safety of Manufactured Nanomaterials*, OECD Environmental Directorate, Paris, France.
(16) Stafforst, T., and Hilvert, D. (2009) Kinetic characterization of spiropyrans in aqueous media. *Chem. Commun.* 287–288.
(17) Aakeröy, C. B., Hurley, E. P., Desper, J., Natali, M., Douglawi, A., and Giordani, S. (2010) The balance between closed and open forms of spiropyrans in the solid state. *Cryst. Eng. Commun. 12*, 1027–1033.
(18) Dowling, A., Clift, R., Grobert, N., Hutton, D., Oliver, R., O'Neill, O., Pethica, J., Pidgeon, N., Porritt, J., Ryan, J., Seaton, A., Tendler, S., Welland, M., and Whatmore, R. (2004) *Nanoscience and Nanotechnologies: Opportunities and Uncertainties*, Royal Society and Royal Academy of Engineering, London, UK.
(19) Abraham, V. C., Taylor, D. L., and Haskins, J. R. (2004) High content screening applied to large-scale cell biology. *Trends Biotechnol. 22*, 15–22.
(20) Davies, A. M., Volkov, Y., and Spiers, J. P. (2008) Drug discovery automation: development of cardiac cell based assays to study drug efficacy and toxicity. *Screening-Trends Drug Discovery 9*, 21–24.
(21) Giuliano, K. A., Haskins, J. R., and Taylor, D. L. (2003) Advances in high content screening for drug discovery. *Assay Drug Dev. Technol. 1*, 565–577.
(22) Abraham, V. C., Towne, D. L., Waring, J. E., Warrior, U., and Burns, D. J. (2008) Application of a high-content multiparameter cytotoxicity assay to prioritize compounds based on toxicity potential in humans. *J. Biomol. Screening 13*, 527–537.
(23) Williams, Y., Sukhanova, A., Nowostawska, M., Davies, A. M., Mitchell, S., Oleinikov, V., Gun'ko, Y., Nabiev, I., Kelleher, D., and Volkov, Y. (2009) Probing cell-type-specific intracellular nanoscale barriers using size-tuned quantum dots. *Small 5*, 2581–2588.
(24) Jan, E., Byrne, S. J., Cuddihy, M., Davies, A. M., Volkov, Y., Gun'ko, Y. K., and Kotov, N. A. (2008) High-content screening as a universal tool for fingerprinting of cytotoxicity of nanoparticles. *ACS Nano 2*, 928–938.
(25) George, S., Pokhrel, S., Xia, T., Gilbert, B., Ji, Z. X., Schowalter, M., Rosenauer, A., Damoiseaux, R., Bradley, K. A., Madler, L., and Nel, A. E. (2010) Use of a rapid cytotoxicity screening approach to engineer a safer zinc oxide nanoparticle through iron doping. *ACS Nano 4*, 15–29.
(26) Byrne, F., Prina-Mello, A., Whelan, A., Mohamed, B. M., Davies, A., Gun'ko, Y. K., Coey, J. M. D., and Volkov, Y. (2009) High content analysis of the biocompatibility of nickel nanowires. *J. Magn. Magn. Mater. 321*, 1341–1345.
(27) O'Brien, P. J., Irwin, W., Diaz, D., Howard-Cofield, E., Krejsa, C. M., Slaughter, M. R., Gao, B., Kaludercic, N., Angeline, A., Bernardi, P., Brain, P., and Hougham, C. (2006) High concordance of drug-induced human hepatotoxicity with in vitro cytotoxicity measured in a novel cell-based model using high content screening. *Arch. Toxicol. 80*, 580–604.
(28) Mingeot-Leclercq, M. P., Brasseur, R., and Schanck, A. (1995) Molecular-parameters involved in aminoglycoside nephrotoxicity. *J. Toxicol. Environ. Health 44*, 263–300.
(29) Reasor, M. J. (1989) A review of the biology and toxicologic implications of the induction of lysosomal lamellar bodies by drugs. *Toxicol. Appl. Pharmacol. 97*, 47–56.
(30) Schins, R. P. F., Lightbody, J. H., Borm, P. J. A., Shi, T., Donaldson, K., and Stone, V. (2004) Inflammatory effects of coarse and fine particulate matter in relation to chemical and biological constituents. *Toxicol. Appl. Pharmacol. 195*, 1–11.
(31) Jones, C. F., and Grainger, D. W. (2009) In vitro assessments of nanomaterial toxicity. *Adv. Drug Delivery Rev. 61*, 438–456.
(32) Kishimoto, T., Akira, S., and Taga, T. (1992) Interleukin-6 and its receptor: A paradigm for cytokines. *Science 258*, 593–597.

TX100123G